Essential Readings in Light Metals: Cast Shop for Aluminum Production.
Edited by John F. Grandfield and Dmitry G. Eskin.

DESIGN OF GRAIN REFINERS FOR ALUMINIUM ALLOYS

A. Tronche and A. L. Greer

University of Cambridge
Department of Materials Science & Metallurgy
Pembroke St., Cambridge CB2 3QZ, UK

Abstract

The efficiency of a grain refiner can be quantified as the number of grains per nucleant particle in the solidified product. Even for effective refiners in aluminium, such as Al-5Ti-1B, it is known from experiments that efficiencies are very low, at best 10^{-3} to 10^{-2}. It is of interest to explore the reasons for such low values, and to assess the prospects for increased efficiency though design of refiners. Recently it has been shown [1] that a simple recalescence-based model can make quantitative predictions of grain size as a function of refiner addition level, cooling rate and solute content. In the model, the initiation of grains is limited by the free growth from nucleant particles, the size distribution of which is very important. The present work uses this model as the basis for discussing the effect of particle size distribution on grain refiner performance. Larger particles (of TiB_2 in the case of present interest) promote greater efficiency, as do narrower size distributions. It is shown that even if the size distribution could be exactly specified, compromises would have to be made to balance efficiency (defined as above) with other desirable characteristics of a refiner.

Introduction

Grain refinement of aluminium alloys has been extensively studied. It is now well demonstrated that the added particles do not behave identically; in particular, at most only 1% of the particles present in the melt are active as nucleation centres [2]. The inactive particles represent a waste of material, and in some cases can be detrimental to the cast product as well as adding to the cost. An ideal grain refiner would ensure a grain structure as fine as possible, and would contain active particles only.

It is considered in this work that the efficiency of a grain refiner is controlled by recalescence of the melt, as initially suggested by Maxwell and Hellawell [3]. These authors modelled grain refinement by considering nucleation on refiner particles as the controlling step, and taking the added particles as identical (i.e. all with the same potency for heterogeneous nucleation and all of the same size). In the present work, the Maxwell and Hellawell approach is modified by taking the initiation of free growth of grains (rather than nucleation as such) to be controlling, and by noting that the refiner particles have a size distribution. Growth proceeds from α-Al caps covering the particles and initiation of free growth occurs (see next section) at an undercooling inversely proportional to particle diameter.

This 'free-growth' model, first reported in [1], has been extensively tested [4] by comparing computed and experimental results obtained with Al-5Ti-1B grain refiner in standard TP-1 tests [5]. The model is now used to consider the efficiency of several hypothetical particle size distributions with the aim of improving refiner design. Predictions are made for the grain size obtained in TP-1 tests if the inoculant particles have a normal distribution of diameter. It is found that the parameters of the normal distributions have a significant effect on the grain size, and that guidelines can be derived for the optimisation of the grain refiners.

The 'Free Growth' model

In this model, following Maxwell and Hellawell [3], the inoculated melt is considered to be spatially isothermal, a reasonable assumption given that thermal diffusion lengths are typically several

cm [4]. The model was developed [1] for Al-Ti-B grain refiners in which the particles are TiB_2 hexagonal platelets treated as discs of diameter d. With such refiners undercoolings as low as 0.01 K have been reported [6]. Classical heterogeneous nucleation theory cannot treat the formation of a nucleus at such low undercooling unless non-physical surface energies are used [7]; an alternative adsorption model has been proposed [8]. Based on microscopical observations [9], it is assumed that the nuclei of α-Al form on the (0001) basal faces of the TiB_2 particles. Once the nucleus is formed, it grows to cover the particle surface but can get thicker only by reducing the radius of curvature of its interface with the liquid - which is unfavourable unless the undercooling is increased. If growth can continue until the solid Al is a hemispherical cap on the face of the TiB_2 particle, then further growth increases the radius of curvature of the solid-liquid interface - a favourable process, 'free-growth', which can proceed without further increase of undercooling. Thus, the hemispherical condition (when the solid-liquid interface has minimum radius of curvature) is the critical barrier for free growth. The critical radius of curvature r^* for which the solid-liquid interface is in unstable equilibrium at a given temperature T is given by

$$r^* = \frac{2\gamma}{(T_l - T)\Delta S_v} \qquad (1)$$

where T_l is the liquidus temperature, γ the interfacial energy between solid and liquid phase and ΔS_v the entropy of fusion per unit volume of aluminium. The critical hemispherical cap on a particle of diameter d in the melt, corresponds to a temperature T, or an undercooling ΔT, at which free growth starts and at which the particle gives rise to new grain:

$$T_l - T = \Delta T = \frac{4\gamma}{d\,\Delta S_v} \qquad (2)$$

Thus, if the number of refiner particles of any size is known, the number of new grains 'nucleated' at any undercooling can be calculated. As the melt is cooled below the liquidus temperature, free growth starts first on the largest particles and proceeds on progressively smaller particles. The free-growth barrier must be significant, because measured nucleation undercoolings substituted in eq. (2) correspond to d values comparable with the larger refiner particles.

The growth of the new grains releases latent heat into the system, slowing the cooling rate. Eventually, the heat release to the system is enough to cause the temperature to rise, which stops the initiation of further grains. A numerical model has been developed in which cooling of the melt is simulated as a series of isothermal steps. At each step, the temperature of the liquid cooled at an imposed cooling rate R, is calculated using a simple heat balance:

$$\frac{T(t) - T(t - \mathrm{d}t)}{\mathrm{d}t} = \frac{Q}{c_v} - R \qquad (3)$$

where Q is the latent heat emitted per unit volume of melt (sum of the heat emitted by the grains nucleated at t and by the growth during the increment dt of pre-existing grains) and c_v the heat capacity per unit volume of liquid Al. The growth of the grains is considered to be spherical (which appears to be a reasonable assumption [1]), and to be diffusion-limited.

The particle size distribution of a commercial Al-5Ti-1B refiner was measured using image analysis of SEM pictures of polished sections. The 'free-growth' model, with this measured distribution as input, was tested against the results of standard TP-1 grain-refining tests. Figure 1 shows the evolution of the measured and computed grain sizes (mean linear intercept) of commercial-purity aluminium with the grain-refiner addition level.

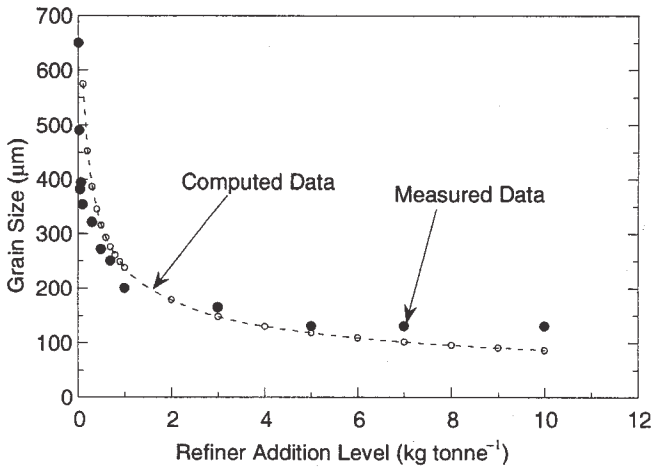

Figure 1: Evolution of grain size with the grain-refiner addition level for commercial-purity Al. The experimental grain sizes measured on TP-1 cones are compared to computed results assuming a cooling rate of 3.5 K s^{-1} in the liquid.

To test the effect of alloy composition, the alloys studied by Spittle and Sadli [10] were considered, the grain sizes were computed and compared to the measured data (Fig. 2). The computed grain sizes match the measured data very well for grain sizes below 400 μm, where the structures are perfectly equiaxed and not columnar [11]. In these experiments, the growth restriction factors $Q = m.C_0.(k-1)$ (m is the liquidus slope, k the coefficient of partition and C_0 the solute concentration in the alloy) cover a large range of values, from less than 1.0 to about 20.0 K.

The comparison in Fig. 1 and Fig. 2 do suggest that when the nucleation is so easy that it is not rate-controlling, the 'free-growth' model successfully predicts the grain size of refined equiaxed aluminium alloys solidified under TP-1 test conditions. The model of course is unable to predict the grain size where there has been settling of the particles, or where there has been poisoning of the nucleation mechanism (for example by Zr [12]).

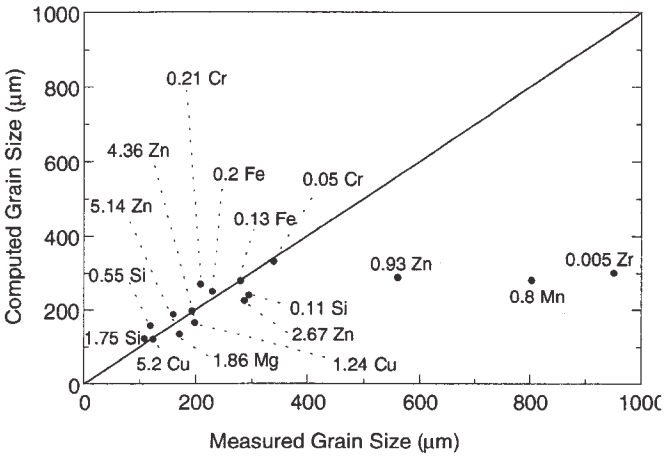

Figure 2: Computed versus measured grain size for a series of alloys. The experimental data were measured by Spittle and Sadli [10] on TP-1 cones inoculated with Al-5Ti-1B at 2 kg tonne^{-1}. The solute content of each alloy (wt%) is indicated on the graph.

The number of grains corresponds to the number of nucleant particles which became active during the solidification. In the above calculations, at most 1% of the particles present in the commercial grain refiner became active. The measured particle size distribution of the commercial Al-5Ti-1B grain refiner and the corresponding active particles are represented in Fig. 3.

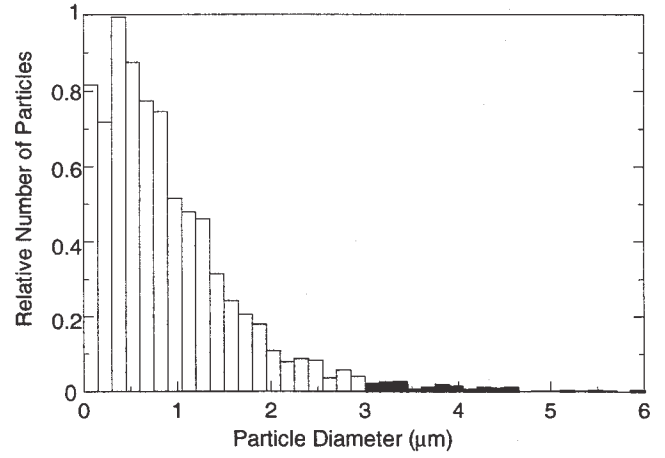

Figure 3: Particle size distribution of a commercial Al-5Ti-1B grain refiner. The 'free growth' model agrees with experimental observations concerning the percentage of active particles (shaded portion).

The 'free-growth' model validated in this way is now used to assess the efficiency of idealised grain refiners with different particle size distributions. An optimised grain refiner should be such that;

- the grain size of the inoculated alloy is as fine as possible,
- a maximum fraction of the added particles become nucleation centres.

The commercial grain refiner would be ideal if the shaded part of the distribution, shown in Fig. 3, were the entire distribution. But such a shape is not practically realisable, and other distributions have to be tested. The calculations have been performed using normal distributions of particle diameters. The effects of the average diameter and the distribution width on the grain-refiner behaviour are assessed.

Efficiency and effectiveness using refiners with normally distributed particle diameters

A fundamental parameter, often quoted, is the *efficiency* defined as the fraction of particles which become active during solidification, i.e.:

$$efficiency = \frac{number\ of\ grains}{number\ of\ added\ particles} \tag{4}$$

However, it should be noted that the objective of grain refinement is to obtain fine grain structures, so that the *effectiveness* of a refiner is more usefully quantified by the grain size at a given refiner addition level; the finer the grain size, the more effective the grain refiner.

Different particle size distributions are tested in this work in order to assess how to optimise grain-refiner performances. Log-normal size distributions are often found in microstructures, but in the present study, normal distributions are considered as a simplification. Such distributions are of the form

$$N(d) = C \exp\left[-\frac{(d-\lambda)^2}{2\sigma^2}\right] \tag{5}$$

where d is the diameter of the particles, λ the mean diameter, σ the width of the distribution and C a constant which represents the number or volume fraction of particles in the grain refiner. For a size distribution $N(d)$, the number of particles N per unit volume and the total volume fraction of particles V_f are respectively equal to :

$$N = \int_{d_{min}}^{d_{max}} N(d)\mathrm{d}d \tag{6}$$

$$V_f = \int_{d_{min}}^{d_{max}} V(d)N(d)\mathrm{d}d \tag{7}$$

where d_{min} is the minimum diameter, d_{max} the maximum diameter and $V(d)$ is the volume of an isolated particle. In this work, the volume of a single particle is taken as the volume of a disc whose thickness is proportional to its diameter ($V(d)=0.3\pi d^3/4$). The minimum diameter d_{min} cannot be negative and is taken as zero. The normal distributions are thus truncated, but this does not significantly affect the total number of particles.

The calculations in this work are performed for a 2 kg tonne^{-1} addition level of Al-5Ti-1B (wt%) refiner to commercial-purity Al (of typical composition given in [4: 9]). With such an addition the total volume fraction of TiB_2 particles in the melt is 3.96×10^{-5}. The grain refiner is taken to have a normally distributed particle size, but the mean diameter λ and width σ of the distribution are varied. For any (λ,σ), the constant C is

$$C\int_{d_{min}}^{d_{max}} \exp\left[-\frac{(d-\lambda)^2}{2\sigma^2}\right]dd = 3.96\times10^{-5} \qquad (8)$$

to retain a constant volume fraction of TiB_2. The number of particles, like C, decreases when λ or σ is increased. In the present case, for example with λ = 0.9 μm and σ = 0.7 μm, $C = 4\times10^{18}$ m^{-3} and $N = 7.8\times10^{12}$ m^{-3}. Figure 4 illustrates some of the distributions used in this work.

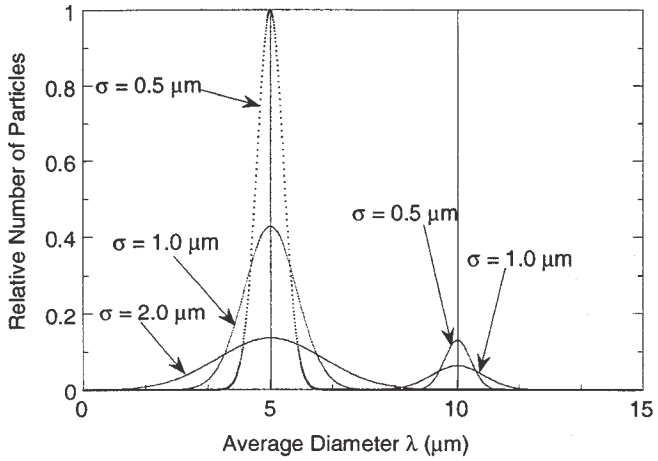

Figure 4: Comparison of some distributions (λ = 5.0 μm and λ = 10.0 μm for different σ values). The area below the distribution represents the number of particles. The volume fraction of particles is fixed and the number of particles decreases sharply when λ increases.

Results

The grain size computed for several particle diameters λ (from 1 μm up to 10 μm) is presented in Fig. 5.

For small λ, the grain size decreases when λ increases, the variation depending strongly on the σ value. Then, the grain size increases steadily with λ. Under the assumed conditions it appears that the refiner is most effective when the average particle diameter is 2 μm. For this λ value the grain size is 50 to 100 μm finer than with a commercial grain refiner.

To understand how the optimum seen on Fig. 5 arises it is useful to consider the efficiency. This has been calculated over the same range of λ for selected σ values (Fig. 6).

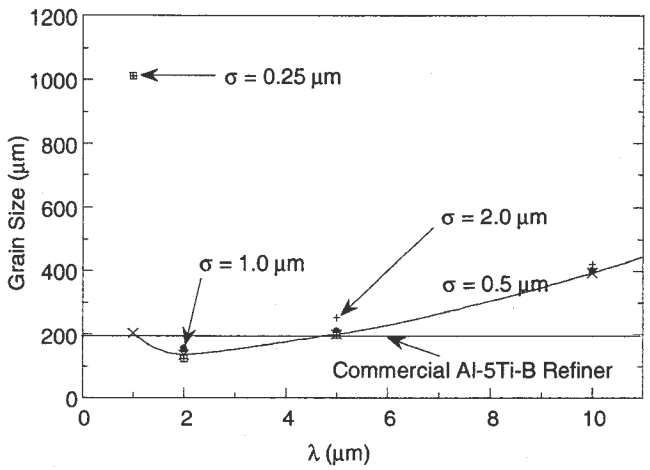

Figure 5 : Evolution of the grain size with average particle diameter λ for distribution width σ as shown. The calculations have been carried out assuming TP-1 conditions (3.5 K s^{-1}) and for a 2 kg tonne^{-1} grain-refiner addition level. The line for σ = 0.5 μm is a guide for the eye. The grain size calculated for a commercial grain refiner is also shown.

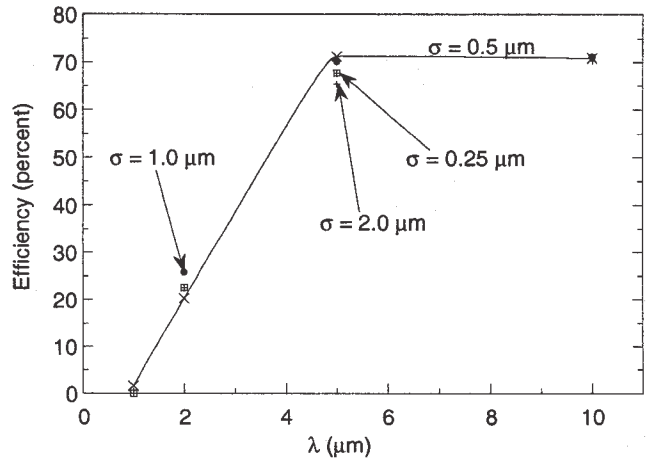

Figure 6: Variation of the refiner *efficiency* with average particle diameter λ for distribution widths as shown. The calculations are for TP-1 conditions (cooling rate = 3.5 K s^{-1}) and at 2 kg tonne^{-1} grain-refiner addition level. The line for σ = 0.5 μm is a guide for the eye.

The fraction of active particles varies from as little as 0.1 % (similar to that found in current industrial practice) to a saturation level of as high as 70%. The marked decrease in *efficiency* as particle size is reduced has two causes. First, smaller size means more particles, and as the trends in Fig. 1 imply, recalescence-limited efficiency is reduced for large populations of particles. Second, smaller size means larger undercooling for initiation of free growth and consequently larger growth rate and faster recalescence. The optimum in effectiveness seen in Fig. 5 arises from the opposing

trends of decreasing efficiency at small particle size and decreasing particle population at large particle size.

It is important to note that even the most efficient refiner gives a grain size only slightly smaller (Fig. 5) than that of a commercial refiner with the size distribution in Fig. 3. Thus the efficiencies of up to 70 % (Fig. 6) are not of practical significance. A high efficiency would be achieved only by (i) eliminating large populations of small, inactive particles, which may not contribute heavily to the overall volume fraction of refiner particles in the melt, and (ii) having a population of particles so low that the grain size is significantly greater than optimum. For the most effective refiner with λ = 2.0 µm (Fig. 5), the efficiency is ~ 20 % (Fig. 6).

The dependence of the effectiveness and the efficiency on the width σ of the particle size distribution have also been studied under the same conditions (2 kg tonne^{-1} addition level, TP-1 test). The variation of the *effectiveness* is reported in Fig. 7.

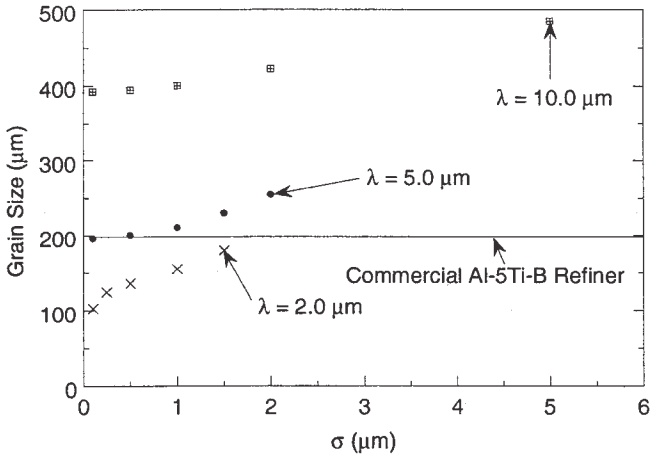

Figure 7: Evolution of the grain size with the width of the particle size distribution σ for different λ values. The calculations are for TP-1 conditions with 2 kg tonne^{-1} grain-refiner addition level.

As seen in Fig. 7, the grain size does not vary much with σ for a given λ value. The general trend is an increase of the grain size with increasing σ. When the width of the distribution increases, early nucleation events are promoted. The grains are bigger and thus release more latent heat, causing recalescence to occur sooner. For the optimum λ value defined in the previous section (2.0 µm), the grain size remains smaller than with a commercial grain refiner for any σ value considered.

The variation of *efficiency* with σ is reported in Fig. 8. For large λ values (~ 10 µm) for which the efficiency is high (~70 %) there is no significant variation with σ. For lower λ values the variation of efficiency is complex but again not very strong. In general it can be concluded that, within the range of parameters studied, refiner effectiveness and efficiency are more sensitive to λ than to σ.

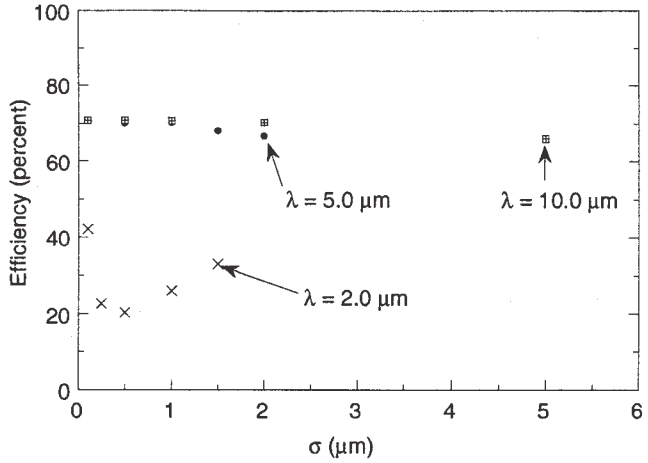

Figure 8: Evolution of the efficiency with the width of the distribution σ, for different λ values. The calculations are for TP-1 conditions and at 2 kg tonne^{-1} grain refiner addition level.

An average grain size as fine as possible may not be the prime concern in grain refinement. Uniformity of grain size through a casting may be of greater importance. Sensitivity of grain size to cooling rate is one way to explore this issue. The variation of grain size with cooling rate is shown in Fig. 9 for idealised grain refiners with varied average particle diameter λ but all with the same distribution width σ. The variation for a commercial refiner (with size distribution in Fig. 3) is also shown for comparison.

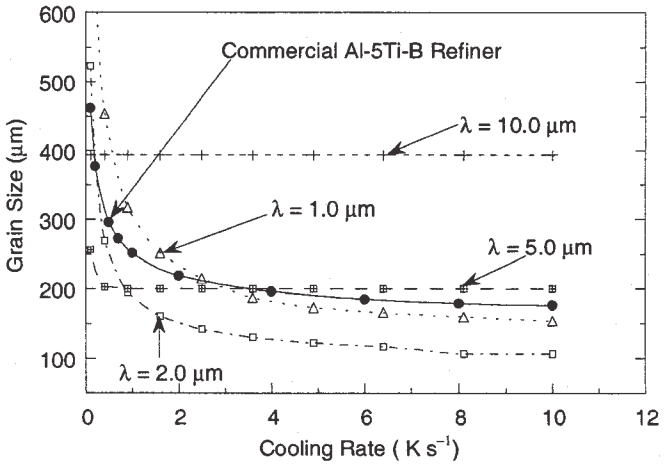

Figure 9 : Evolution of the grain size with the cooling rate for idealised grain refiners with different average diameters and for a commercial grain refiner.

While greater λ values give coarser grain sizes, they also confer useful insensitivity to cooling rate. For example with λ = 1 µm, the grain size varies greatly with cooling rate, from 900 µm at 0.1 K s^{-1} to a plateau of about 150 µm at high cooling rate. The variation decreases when λ increases, from 500 µm to 100 µm for λ = 2 µm, and from 300 µm to 200 µm for λ = 5 µm. For the commercial grain

refiner the variation is from 460 μm at 0.1 K s^{-1} to 175 μm at high cooling rate, which is about twice greater than the variation observed for the optimised grain refiner.

Conclusions

The 'free-growth' model, based on the Maxwell-Hellawell analysis of grain refinement, takes the size distribution of the added particles into account. It successfully predicts experimental grain sizes obtained under TP-1 conditions, and the low efficiency of commercial refiners (at most 1%).

The model was used to predict the behaviour of an idealised grain refiner with a normal distribution of particle diameter. For different distributions (varying average diameter and distribution width), the addition level of the grain refiner is kept constant, equivalent to 2 kg $tonne^{-1}$ of the commonly used Al-5Ti–1B. The model results may help in designing better grain refiners, by assessing the efficiency and the effectiveness of the different distributions under TP-1 conditions. It was shown that:

- Refiner performance is improved for narrower particle size distributions. However the width σ of the distribution does not have a dominant influence for a realistic range σ.
- The average particle diameter λ in the refiner is particularly important. Within the conditions tested, an average diameter of 2 μm gives the minimum grain size. However the sensitivity to cooling rate decreases with increasing λ. With λ = 5 μm there is a good combination of fine grain size and relative insensitivity to cooling rate.
- Efficiency may be a misleading guide to refiner effectiveness. Commercial grain refiners give close to the best achievable (i.e. minimum) grain size despite having very low (10^{-2} to 10^{-3}) efficiencies. The inactive particles in such refiners, though numerous, do not constitute a dominant volume fraction of the particle phase.
- An optimised refiner, with greater efficiency than the present commercial refiners, would give a small decrease in grain size, but a large decrease in the number of refiner particles swept into the intercellular liquid during the final stages of solidification. The consequences of differing populations of particles at that stage of solidification (for example on the selection of second-phase intermetallics [13]) remain to be fully explored.

Acknowledgements

AT acknowledges financial support from the London & Scandinavian Metallurgical Co. Ltd. and Pechiney (CIFRE studentship), and useful discussions with D. J. Bristow, A. Hardman and M. A. Kearns at LSM and L. Maenner and P. Jarry at Pechiney Centre de Recherche de Voreppe.

References

1. A. M. Bunn, P. V. Evans, D. J. Bristow and A. L. Greer, "Modelling the effectiveness of Al-Ti-B refiners in commercial purity aluminium," Proc. Conf. 'Light Metals 1998', ed. B. Welch (Warrendale, PA: TMS, 1998), 963-968.

2. D. G. McCartney, "Grain-Refining of Aluminium and its Alloys using Inoculants," Inter. Mater. Rev., 1989, **34**, 247-260.

3. I. Maxwell and A. Hellawell, "A simple model for grain refinement during solidification," Acta Metall., 1975, **23**, 229-237.

4. A. L. Greer, A. M. Bunn, A. Tronche, P. V. Evans and D. J. Bristow, "Modelling of grain refinement by inoculation of metallic melts", paper submitted to Acta Mater.

5. Aluminium Association Standard Test Procedure for Aluminium Grain Refiners 1990, TP-1, The Aluminium Association, Washington D.C. 20006.

6. L. Backerud and S. Yidong, "Grain-refining mechanisms in aluminium as a result of additions of titanium and boron, Part 1," Aluminium, 1991, **67**, 780-785.

7. N. Marasli, J. D. Hunt, "The use of measured values of surface energies to test heterogeneous nucleation theory", J. Cryst. Growth, 1998, **191**, 558-562.

8. W. T. Kim and B. Cantor, "An adsorption model of the heterogeneous nucleation of solidification", Acta Metall. Mater., 1994, **42**, 3115-3127.

9. P. Schumacher, A. L. Greer, J. Worth, P. V. Evans, M. A. Kearns, P. Fisher and A. H. Green, "New studies of nucleation mechanisms in aluminium alloys: implications for grain refinement practice", Mater. Sci. Technol., 1998, **14**, 394-404.

10. J. A. Spittle and S. Sadli, "Effect of alloy variables on grain refinement of binary aluminium alloys with Al-Ti-B", Mater. Sci. Technol., 1995, **11**, pp. 533-537.

11. S. Sadli, PhD thesis, University College of Swansea, 1993.

12. A. M. Bunn, P. Schumacher, M. A. Kearns, C. B. Boothroyd and A. L. Greer, "Grain refinement by Al-Ti-B alloys in aluminium melts: a study on the mechanisms of poisoning by zirconium", Mater. Sci. Technol., 1999, **15**, pp. 1115-1123.

13. M. W. Meredith, A. L. Greer and P. V. Evans, "The influence of grain refiner on intermetallic phase selection in dilute Al-Fe alloys", Solid. Processing 97, ed. J. Beech and H. Jones, 1997, 541-545.